International Journal of Concrete Structures and Materials
Vol.18, No.3E, pp.173~181, December 2006

Correlation between Analytic and Experimental Results on Inelastic Behavior of Reinforced Concrete Frame

Han-Seon Lee[1)], Sang-Dae Kim[2)], Cheol-Yong Park[3)], and Dong-Woo Ko[2)]

(Originally published in Korean version of ***Journal of KCI***, Vol.9, No.6, December 1997)

Abstract: The objectives of this study are to evaluate the reliability of an existing nonlinear analysis program for predicting the inelastic behavior of reinforced concrete frame with seismic details and to observe the redistribution of the internal forces, which can not be easily measured by an experiment. In order to carry out this task, the nonlinear analysis program of IDARC 2D(3) was run on a 2-bay, 2-story moment-resisting reinforced concrete plane frame with seismic details. (1) The effort to obtain the results of the analysis similar to those of experiment was made by determining the appropriate values of model parameters. The comparison of the analysis results with those of experiment and the observation of the distribution of internal forces obtained through nonlinear analysis points to the following conclusions. (1) The overall relationship between lateral load and lateral displacement given by the analysis is similar to that of experiment. However, the values of initial stiffness and the amount of energy dissipation in the initial displacement steps given by the analysis show larger values than those of experiment. (2) The analysis provided detailed information on the distribution and redistribution of internal forces and proved useful in elucidating the crack pattern, the sequence of the occurrence of plastic hinges, and the failure or yielding mechanism for the whole structure. (3) In spite of the similarity in overall behavior of analysis and experiment, there exists a significant discrepancy in some local behaviors. Furthermore, the hysteresis in the relationship between moment and curvature in some column ends have shown sudden deteriorations in strength, which can not be interpreted satisfactorily at the present time. Therefore, it is necessary to develop a better analytical model to fill this knowledge gap.

Keywords: nonlinear analysis, reinforced concrete, moment-resisting frame, analytical model

1. Introduction

Most reinforced concrete structures are damaged due to nonlinear deformation under severe earthquake. The prediction for the damage and collapse of the structures to ensure the structural safety is very important. Recently, minor earthquake have occurred over 20 times a year in Korea. These recent earthquakes indicate that the Korean Peninsular is no longer safe from seismic hazard. Thus, the need for investigating the non-linear structural response of the structures under earthquake is increasing gradually.

From this necessity, the response of structures under large earthquake has been predicted or examined by analytic methods. However, these analytical methods should be verified experimentally in order to prove its reliability. On the other hand, most of the data obtained from the experimental measuring devices are deformation and displacement, and precise load cells must be installed in the appropriate location to measure the change in the distribution or redistribution of internal forces, etc. This can cause the concern for the increase in the incidental experiment cost and the change in the behavior of the structure itself. Thus, the experimental data have their own limitations in terms of the quantitative and qualitative perspective. Analytical methods are used to supplement these limitations. This study uses IDARC 2D program,[3] which was developed at the State University of New York at Buffalo in the USA, to predict the non-linear behavior of the moment-resisting reinforced concrete plane frame, and then the analytical results are compared with the experimental results to assess the reliability of the analytical program for its application to the moment-resisting R/C (reinforced concrete) plane frame with seismic details.

As aforementioned, the 2-stories R/C plane frame with seismic details is selected, and a quasi-static experiment is carried out by controlling the roof displacement as shown in Fig. 1. The details of this experiment can be referred to in the reference.[1] Additionally, the redistribution of the internal forces and the process of forming plastic hinges are observed and reported with the intention of supplementing the analysis of the experimental data.

Many researchers have investigated the seismic behavior using IDARC 2D program up until now. Kunnath et al. (1991) showed that the results of the IDARC 2D and DRAIN 2D[1]

[1)] KCI member, Dept. of Architectural Engineering, College of Engineering, Korea University, Seoul 136-705, Korea. *E-mail: hslee@korea.ac.kr*
[2)] KCI member, Dept. of Architectural Engineering, College of Engineering, Korea University, Seoul 136-705, Korea.
[3)] Ssangyong Institute of Construction Technology, Seoul 138-726, Korea.

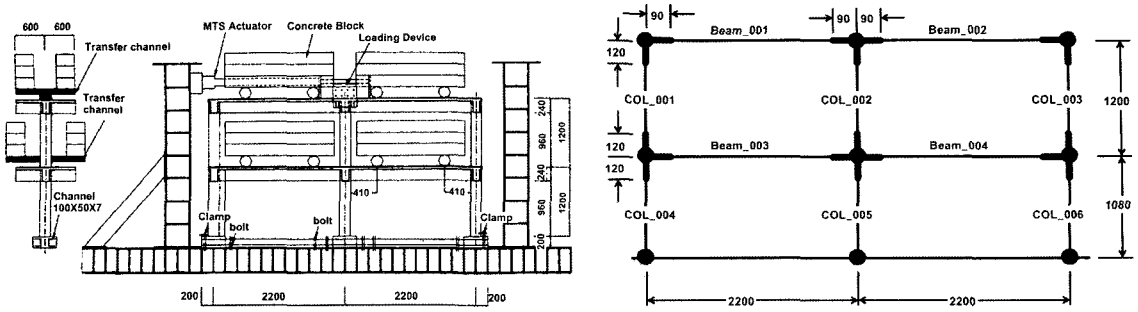

(a) Experiment (b) Analysis

Fig. 1 Geometry and dimension of structure. (unit : mm)

analyses of the displacement in the two-story structures due to the earthquake at Taft (1952, N69W) were similar,[5] and investigated the relationship between the results of the lateral loading and unloading experiment on 2-bay, 3-story R/C frame and the results of IDARC 2D analysis.[7] Roufaiel et al. (1987)[8] compared the results of vibration table test for 2-story R/C frame reduced to half the size and the IDARC 2D analysis.

The analysis process of IDARC 2D program is described in the following section 2. Section 3 compares the experimental results with the results of IDARC 2D program analysis on a 2-bay, 2-story R/C plane frame. Finally, a non-linear analysis is used to describe the process of redistribution of the internal forces, which can not be obtained through an experiment, in section 4.

2. Determination of the analytical model

2.1 Structural model

Fig. 1 shows the geometry and the dimension of specimen. In Fig. 1(b), the length of the member indicates the distance to the center of the joint, and the rigid zone at each connecting point is marked with a thick line.[1]

2.2 Models for the materials

The average compressive strength of the concrete was 33 MPa, and the average yield strength of the reinforcing bar was 372 MPa.[2]

The story drift predicted by analysis was lower than that of actual experimental result. Thus, this factor was adjusted a little higher, and the values as the same as the experimental result are given in the figure. Here, Hognestad model was applied to the concrete up to the ultimate compressive stress, and Modified Kent and Park model was applied to the concrete in consideration of the influence of hoop and stirrup after the ultimate compressive stress. Trilinear model, which considers yielding and softening of the deformation, was applied to the reinforcing bar.[1]

2.3 Cross-sectional model

Fig. 2 depict the geometry and dimension of column and beams of specimen. Column section in analytical model adopted the same section in experiment, but beam section is adopted T-shaped beam with 505 mm of effective was used initially pursuant to ACI 318-89. However, the effective width was adjusted a little to 552 mm in order to make the analysis result and experimental result to concur with each other as shown in Fig. 2 (b).

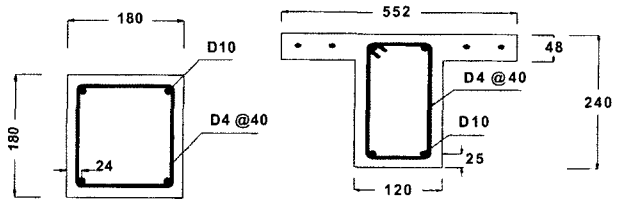

(a) Column (b) Beam

Fig. 2 Geometry, dimension and detail of sections. (unit : mm)

Using these cross sections, the IDARC 2D analytical program determines the model of moment-curvature envelope relationship for the cross sections of the column and beam. Because the cross sections of the column and beam are rectangular and T-shaped, respectively, the cross sectional models for the former and the latter are depicted as a symmetrical trilinear curve as shown in Fig. 3 (a) and a non-symmetrical trilinear curve as shown in Fig. 3 (b).

2.4 Hysteretic behavior model

A element model, which assumed the flexibility distribution as linear, was selected in order to compute the energy dissipation capacity of each member, and the relationship between moment and angle of rotation at both nodes (joints) of the member was derived.[5,6]

The relationship between major cross sectional force and deformability of the member can be illustrated as a hysteretic curve. To determine the hysteretic curve model for the analysis, the initial hysteretic curve is assumed to be the trilinear curves of Fig. 3 for beam and column, and the effects of stiffness degradation, strength deterioration, and pinching on the hysteretic curve are considered for both cases of lateral loading and unloading.[7]

The stiffness degradation can be expressed by the following procedure as depicted in Fig. 4. From the trilinear curve of cross sectional model, a extended line is drawn in the opposite direction to the first inclination. Then, a straight line is drawn parallel to x-axis using the assumed values of multiplying a random multiplier, α, to the yield moment of the cross section. The crossing point of the two straight lines is designated A, the common (target) point. Then, assuming the curve at the unloading step runs from the maximum or minimum value toward this point A until it crosses the x-axis, the stiffness degradation is thereby expressed.

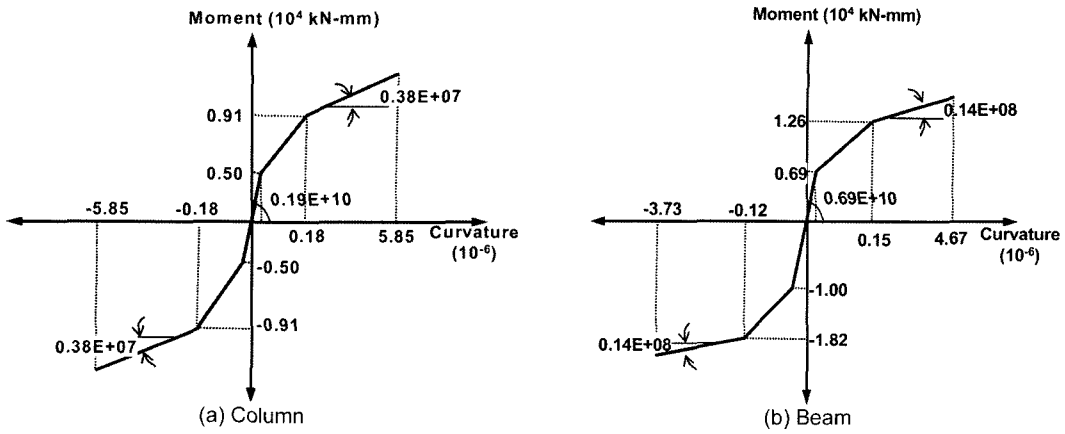

Fig. 3 Moment-curvature envelope curves.

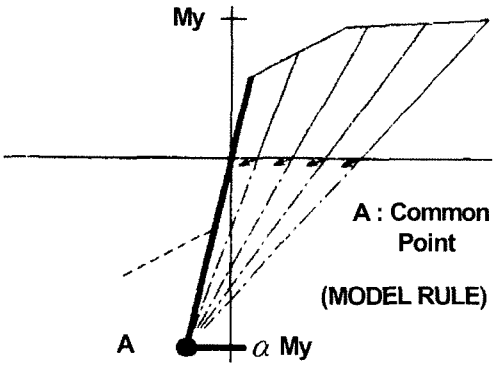

Fig. 4 Stiffness degradation effect.

Pinching effect can be expressed by the following procedure as shown in Fig. 5. A random multiplier, γ, is multiplied to the yield moment of the cross section. After the value is reduced, a straight line is drawn parallel to x-axis. The crossing point of this straight line and the straight line at the unloading step is designated A, the crack closing (target) point. Then, the curve at the reloading step runs until it crosses with the vertical line from the point A in Fig. 5. Assuming that the curve runs toward the previous maximum or minimum value afterwards, the pinching effect can be determined. Using this pinching effect, the effect of reducing energy dissipation of the hysteretic curve can be expressed.

The strength deterioration effect can be determined by the following procedure as shown in Fig. 6. Assuming that the load is removed after reaching the maximum value (indicated by point A, actual maximum load point) and then the hysteretic curve runs toward a random target point B (indicated by point B, artificial maximum load point), which is larger than the previous maximum load point (A) at reloading step, the hysteretic curve at the reloading step is extended to its crossing point (indicated by point C) with the vertical line from maximum strain (ϕu). The load is removed again at this point C. This strength deterioration effect can be considered in terms of strength and energy. The strength aspect of the strength deterioration can be computed by the degree of reduction from A to C. The energy aspect of the strength deterioration effect can be computed by comparing the area formed by the closed hysteretic curve past the point A and the area formed by the closed hysteretic curve past the point C.

Using the above principles, the hysteretic curve used in the analysis can express the stiffness degradation effect, strength deterioration effect, and pinching effect by determining each parameter value as shown in Fig. 7.[3]

Here, the stiffness degradation effect decreases as the variable, HC (α), gets larger, and this means that the inclination of the second cycle is almost the same as the initial inclination. The strength deterioration effect can be considered from the aspects of strength and energy as aforementioned. The variable HBD of the strength aspect of the strength deterioration has the value of zero if the hysteretic curve of the second cycle is the same as the maximum or minimum value of the previous cycle. The value for this variable can be increased by the degree of strength deterioration. The value for the variable HBE of the energy aspect is determined by the area inside the hysteretic curve. Likewise the case of the strength aspect of the strength

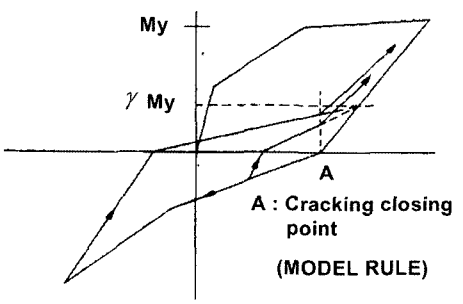

Fig. 5 Pinching effect.

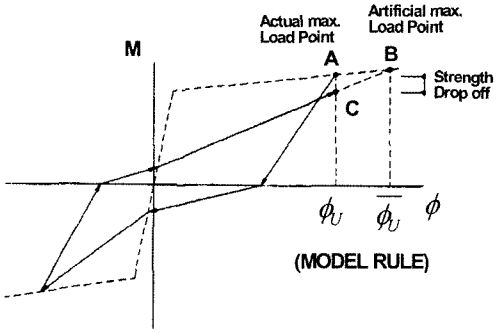

Fig. 6 Strength deterioration effect.

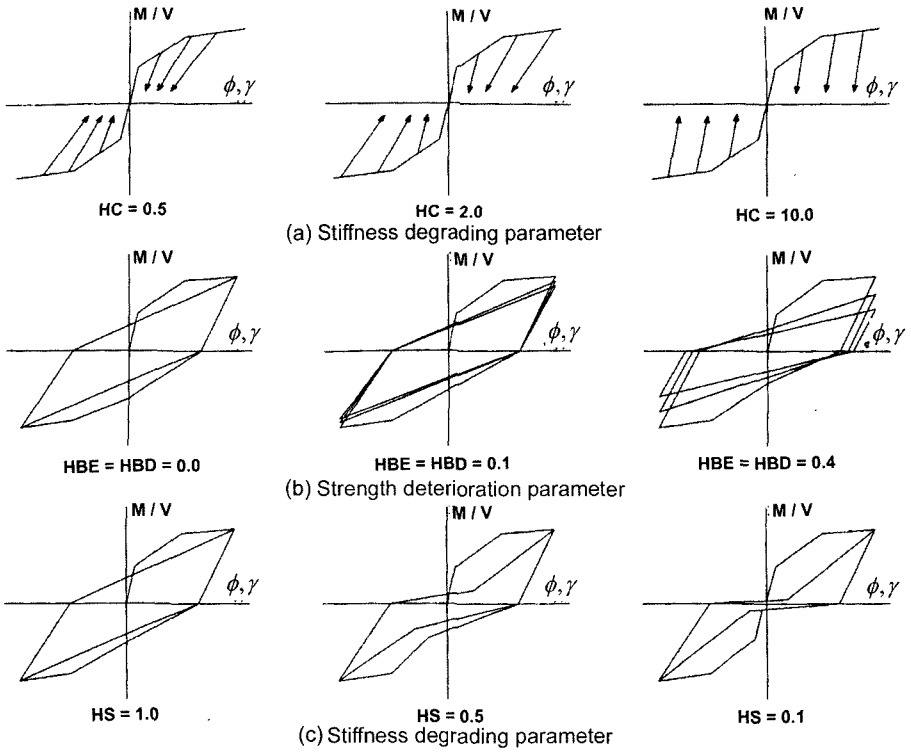

Fig. 7 Three parameters of hysteretic model for analysis.

Table 1 Parameters of hysteretic used in the analysis.

Type	Stiffness degradation	Strength deterioration		Pinching effect
	HC (α)	HBD	HBE	HS (γ)
Factor	6.0	0.0	0.05	1.0

deterioration, it has the value of zero if the area inside the hysteretic curve does decrease, and its value can be increased by the degree of energy deterioration. The parameter for the pinching effect varies from 1.0 to 0.1 by the degree of reduced inclination. The parameters of the hysteretic behavior model used in this analysis are shown in Table 1. These parameters are selected so that they are the closest to the experimental results based on the heuristic approach of trying out various values for the parameters, and there is no theoretical basis for the selection.

3. Correlation between the analysis results and experimental results

The analytical model determined by the above procedure was applied to the specimen illustrated in Fig. 1. Fig. 8 shows the lateral roof displacement history used in experiment and quasi-static analysis.[2,3] The parameters were adjusted to make the analysis result as similar as possible to the experimental result, and the correlation between the experimental result and obtained analysis result was examined.

3.1 Relation between lateral load and lateral displacement

The relation between lateral load and lateral displacement as obtained from the experiment and analysis is illustrated in Fig.

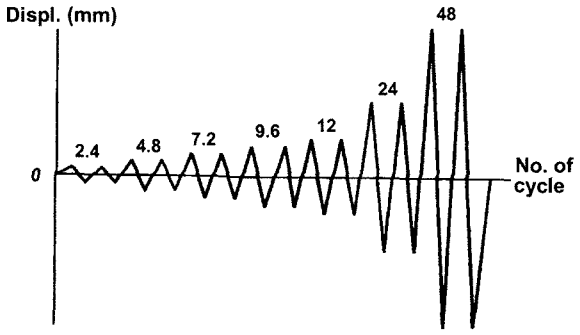

Fig. 8 Lateral displacement history at roof.

9. Examining the relationship with respect to the stiffness, the initial stiffness of the analysis result is somewhat greater, and the stiffness degradation at the second cycle was about the same for both results. With respect to the strength deterioration, the initial strength of the analysis result was somewhat greater,

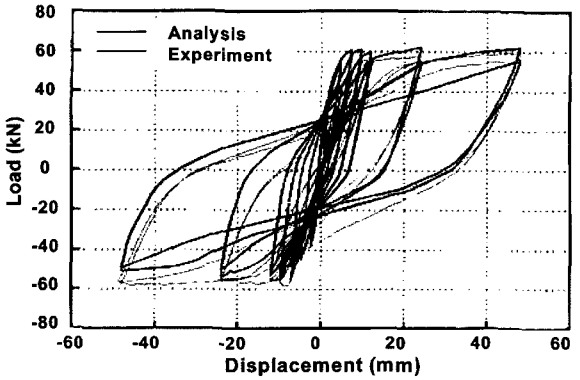

Fig. 9 Lateral load-lateral displacement relation.

but the strength of the analysis result subjected to loading step at the negative (−) direction was a little smaller than the strength of the experimental result. Moreover, the strength deterioration effect at the second cycle was somewhat more conspicuous for the analysis result (Fig. 10). With respect to the yield effect, although the experimental result showed a symmetrical pattern for the positive (+) and negative (−) direction, the analysis result did not exhibit a clear yield effect at the step subjected to loading at the negative (−) direction.

Figs. 10-a and 10-b compare the variation in strength and stiffness, respectively, of the experimental result and analysis result stepwise by lateral displacement. The stiffness in Fig. 10-b was computed by the ratio of the load to the maximum displacement at each step of lateral displacement change. Fig. 11 shows that analysis exhibits noticeable energy dissipation already even at the early step compared to the energy dissipation of the experimental result. That is, the energy dissipation of the analysis result was noticeably greater than that of the experimental result up to the fifth step (12.0 mm) of the lateral displacement change. Nevertheless, the yield effect was observed for both experimental and analysis results at the third step (7.2 mm) of the lateral displacement change and the fourth step (9.6 mm) of the lateral displacement change.

3.2 Relation between lateral load and story drift

Figs. 12 and 13 illustrate the lateral load-drift relation for the first and second story, respectively. As it can be seen in Fig. 12, the drift at the first story of the analysis result is relatively greater than that of experimental result. Accordingly, the drift at the second story of the analysis result was smaller than that of the actual experimental result. This can be explained by the following reasoning. While inelastic behavior was concentrated at the second story due to the soft story failure mechanism after the step of the lateral displacement of 12.0 mm in the experiment, there was relatively less concentration of inelastic behavior at the second story in the analysis model due to the

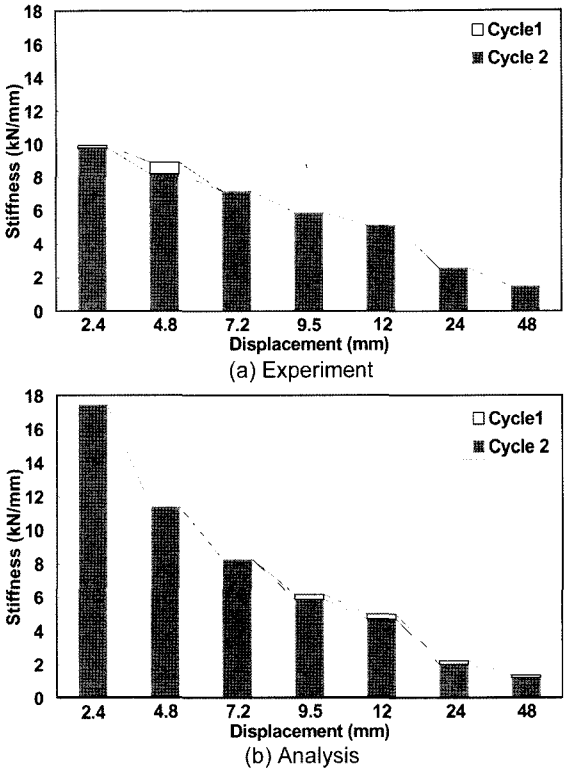

Fig. 10-b Comparison of stiffness.

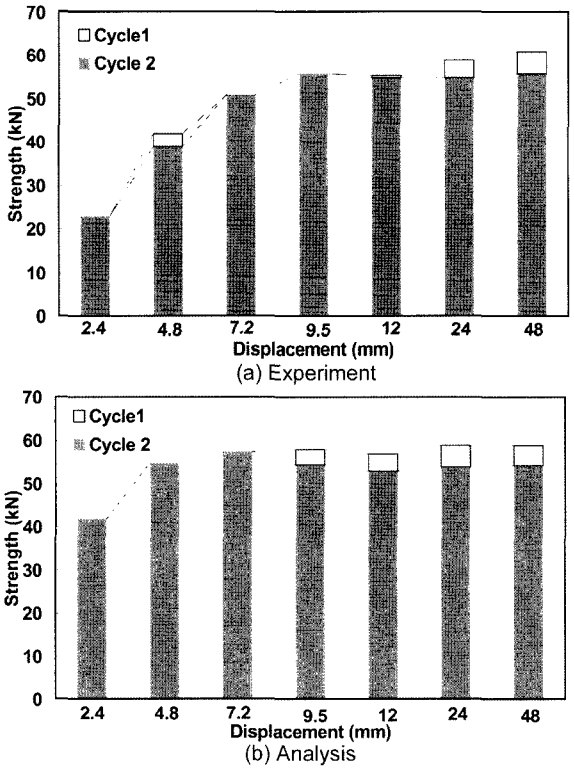

Fig. 10-a Comparison of strength.

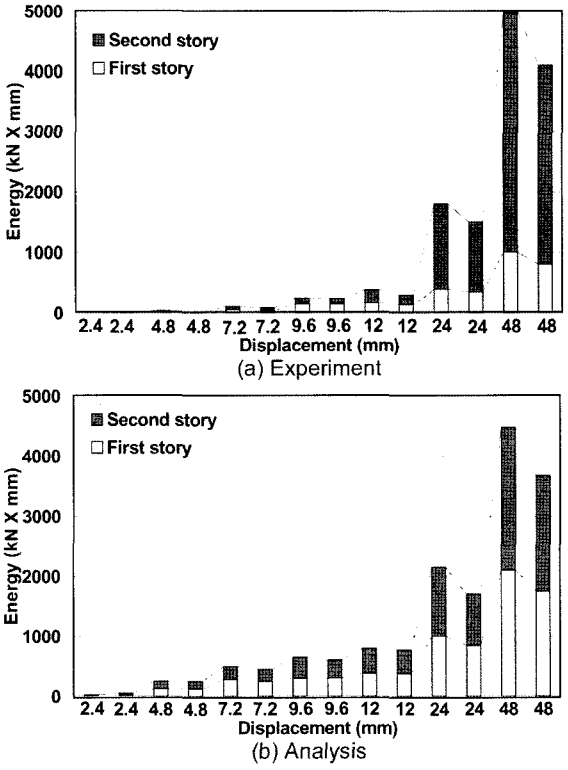

Fig. 11 Energy dissipation capacity.

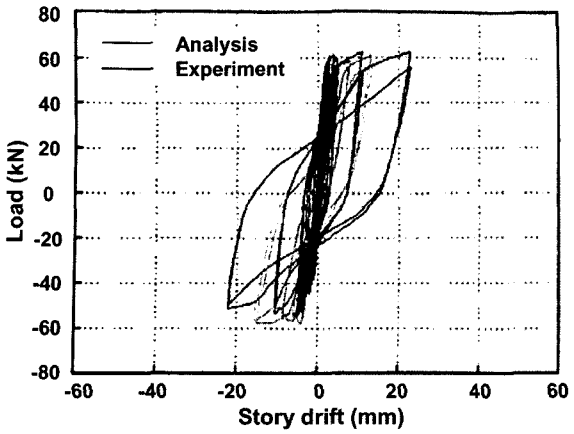

Fig. 12 Lateral load-story drift at first story.

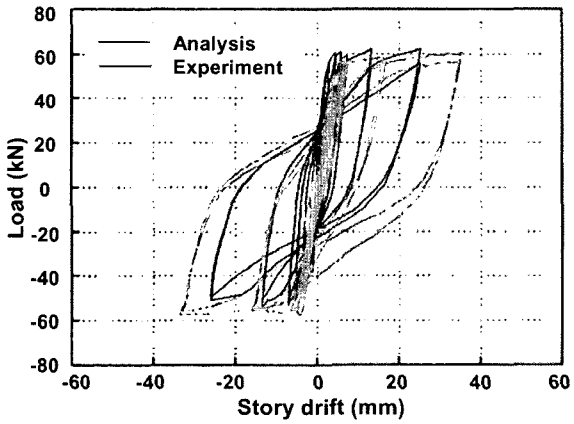

Fig. 13 Lateral load-story drift at second story.

fact that the final failure mechanism was manifested at the step of the lateral displacement of 24.0 mm. Thus, it was found from this difference that it would be very difficult to describe the inelastic behavior of the actual structure accurately only with the variables of the model given by the analytic program.[3]

3.3 Relation between lateral load and angle of rotation

The possible location of plastic hinge in the beam was predicted, and the device for measuring the angle of rotation in the beam was installed as shown in Fig. 14. Then, the analysis involved calculating the curvature at both connecting nodes at the rigid zone as shown in Fig. 15. Assuming that this curvature varied linearly with the length of the member, a straight line was drawn between the connecting nodes to compute the areas of the trapezoids marked by oblique lines. The angle of rotation was assumed to occur from these areas.

The relation between lateral load and angle of rotation for the beam was obtained by this method. The typical results are compared in Figs. 16 and 17. It can be seen from the figures, the analysis result concurred fairly well with the experimental result. The Fig. 16 shows that the energy dissipation at the left of the left beam at the first story, which exhibits yielding, was greater for the analysis than for the experiment. Nevertheless, the overall trend of inelastic behavior was almost the same for both the analysis and experiment.

The possible location of plastic hinge in the column was

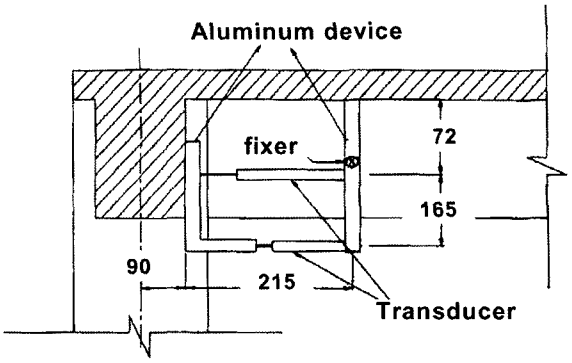

Fig. 14 Device set-up to measure the angle of rotation in beam. (unit : mm)

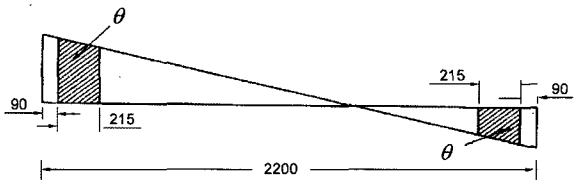

Fig. 15 Calculation of the angle of rotation in beam from analysis.

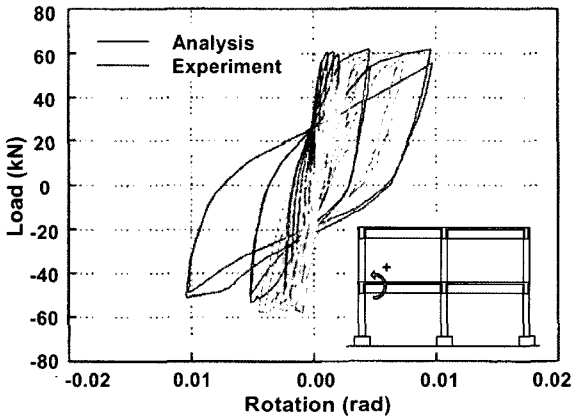

Fig. 16 Angle of rotation in the left of left beam at first story.

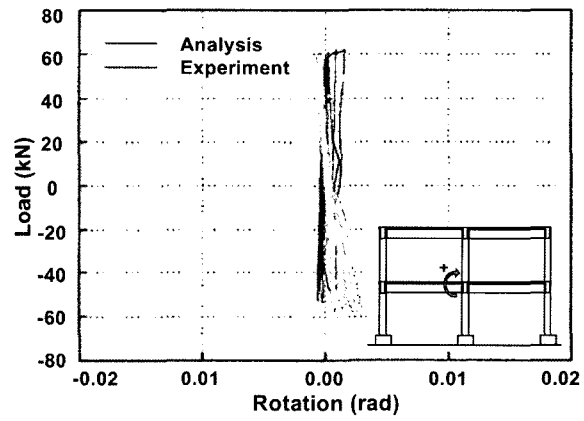

Fig. 17 Angle of rotation in the right of left beam at first story.

predicted, and the device for measuring the angle of rotation in the column was installed as shown in Fig. 18. It should be pointed out that most of the major cracks occurred at the joint of the beam and column during the actual experiment, and the

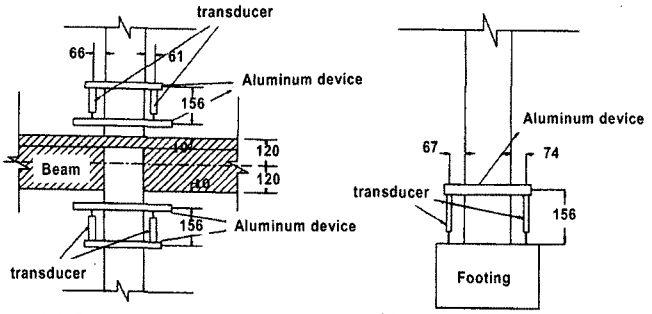

(a) Beam-column joint (b) Column-footing joint

Fig. 18 Device set-up to measure the angle of rotation in column.

measuring device capture them. Thus, the angle of rotation obtained from the experiment could not reflect the plastic rotation angle at the ends of the actual column. Likewise with the case for the beam, the analysis method to compute the rotational angle of column involved calculating the curvature at both connecting nodes at the rigid zone as shown in Fig. 19. Assuming that this curvature varied linearly with the length of the member, a straight line was drawn between the connecting nodes to compute the areas of the trapezoids marked by oblique lines. The angle of rotation was assumed to occur from these areas. The relation between lateral load and angle of rotation for the column member was obtained from this method. The typical results are compared in Figs. 20 and 21. It can be seen from the hysteretic curves in the figures, the analysis result concurred fairly well with the experimental result. However, the stiffness of the analysis result was generally greater than that of the experimental result. Additionally, with respect to the yielding member, the energy dissipation was greater for the analysis than for the experiment. Nonetheless, the result of the experiment measuring the reinforcement strain with a gauge revealed that the reinforcement bars around the gauge yielded as shown in Fig. 22. Thus, it can be construed that the analysis result is valid to a certain extent, but it does not entirely reflect the experimental result accurately.

4. Analysis of the distribution of internal forces based on analysis results

Fig. 23 shows the distribution of moment by displacement stepwise. Here, each number represents the ratio of maximum moment to the yield moment for each cross section. The ratios

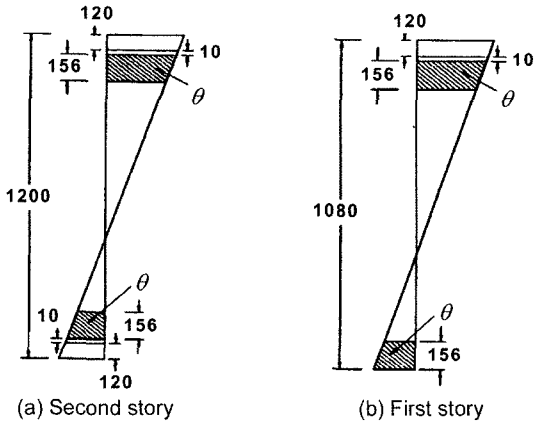

(a) Second story (b) First story

Fig. 19 Calculation of the angle of rotation in column from analysis.

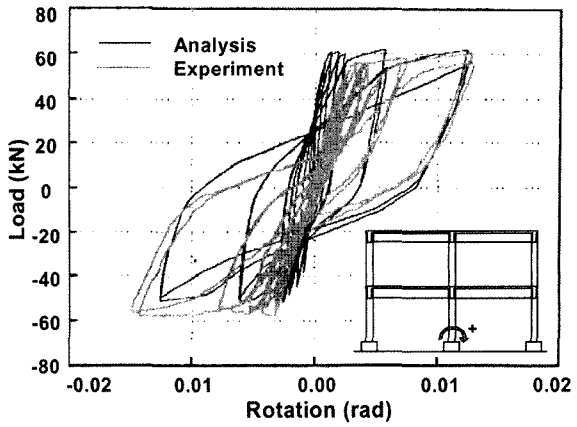

Fig. 20 Angle of rotation in the bottom of middle column at first story.

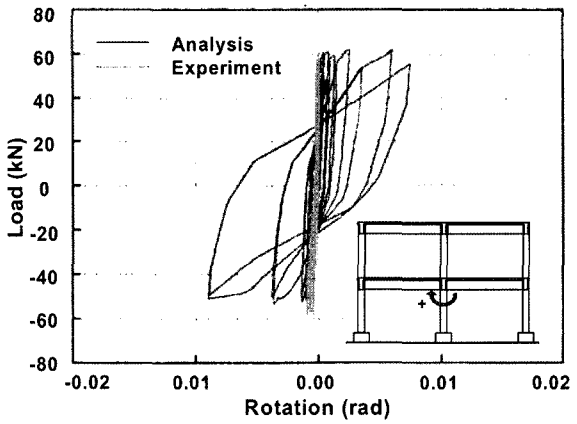

Fig. 21 Angle of rotation in the top of middle column at firs story.

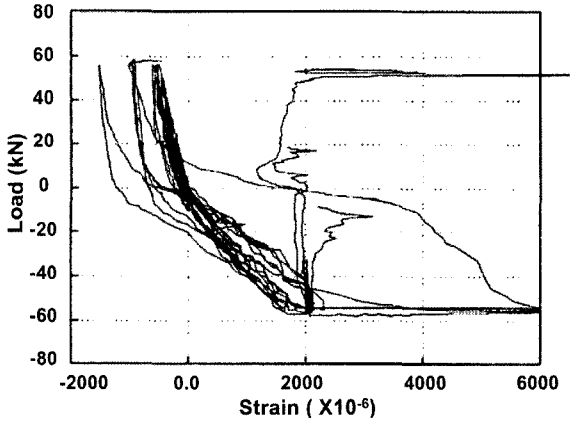

Fig. 22 Relation between load and reinforcement strain in the top of middle column at first story.

for the beam member and the column member are shown inside the rectangle and italic style, respectively. The symbol × indicates the plastic hinge with the occurrence of yielding, and the symbol ● represents the place of previous occurrence of yielding. Using this analysis result, the occurrence of plastic hinge in the experimental structure and the occurrence order and the final occurrence of plastic hinge by the analysis are shown in Fig. 24. It can be seen from the figure that, although it is difficult to

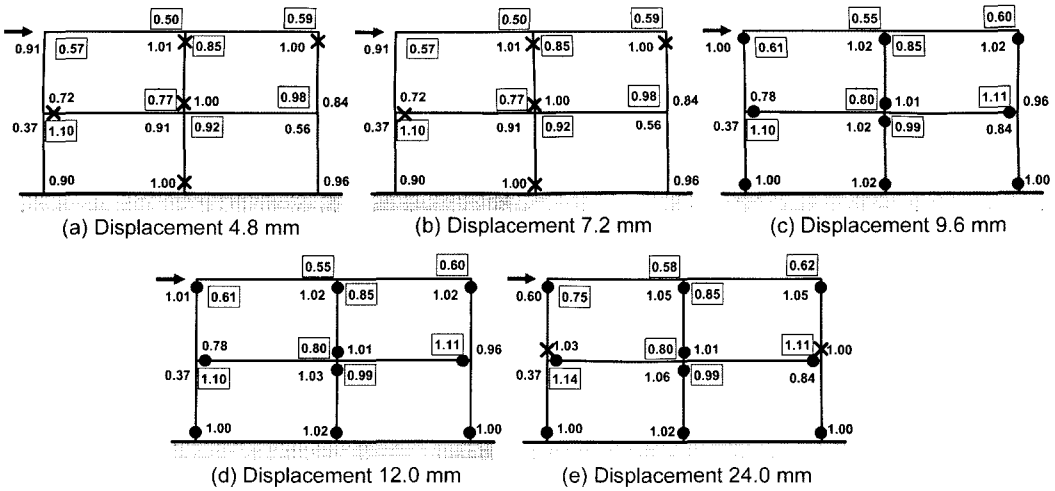

Fig. 23 Occurrence of plastic hinges in each displacement (●: Old, ×: new).

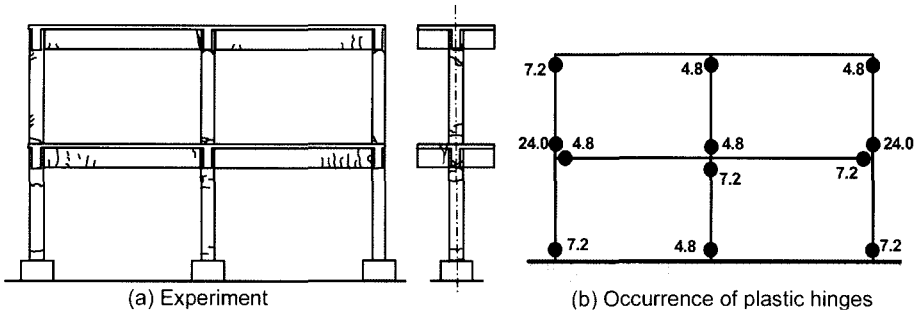

Fig. 24 Comparison of the failure mechanisms between experiment and analysis.

obtain the analysis result in complete concurrence with the experimental result, determination of the analytical model, which can derive the behavior similar to the experimental behavior analytically, is possible to a certain extent.

5. Conclusions

In the discussion above, the reliability of the analytical model was evaluated through the correlation between the result calculated from an analytical model of existing non-linear behavior analysis program and the result of the actually carried-out experiment. The distribution of the internal forces of the member, which could not be obtained by an experiment, was derived from the above analysis. The conclusions derived so far are presented as it follows.

(1) Each hysteretic curve obtained by the analysis generally showed the trend similar to the experimental result with respect to the stiffness, strength, energy dissipation capacity, etc.

(2) However, the relation between lateral load and lateral displacement showed that the analysis result was noticeably larger than the experimental result with respect to the initial stiffness and strength. Likewise, the energy dissipation of the analysis result was initially greater than that of experimental result. Moreover, there was a significant difference in the lateral load-story drift relation between the analysis result and the experimental result.

(3) In addition, the analysis result revealed a rapid strength deterioration effect partially or a small energy dissipation behavior based on the relationships of moment-angle of rotation and moment-curvature. This finding was different from the actual experimental result, and this analysis result also brought about the partial difference in the overall relationship of lateral load-lateral displacement after all. This shortcoming of the analytic model means it needs to be revised and supplemented through the development of a more appropriate model in the future.

(4) The analysis result computed the location of the occurrence of the plastic hinge as the same as that of the actual experimental result. The order of the occurrence of the plastic hinge as computed by the analysis model was to start from the bottom of the column at the first story and then to spread to the top of the column at the first story and the beam member. Finally, the analysis predicted yielding at the bottom of the column at the second story to result in the failure mechanism. This analysis result was in concurrence with the experimental result.

References

1. Lee, H. S. and Woo, S. W., "Repetitive Lateral Loading Experiment on a 2-Bay, 2-Story Reinforced Concrete Frame," *Journal of Korea Concrete Institute*, Vol.8, No.6, 1996, pp.195~204.

2. Lee, H. S. and Woo, S. W., "Experimental Study on Analogy of Structural Behavior of a Reinforced Concrete Miniature Model," *Journal of Korea Concrete Institute*, Vol.8, No.6, 1996, pp.183~193.

3. Reinhorn, A. M., Kunnath, S. K., and Valles-Mattox, R.,

IDARC 2D Version 4.0: A Program for the Inelastic Damage Analysis of Building, USER'S MANUAL, 1996.

4. Park, R. and Paulay, T., *Reinforced Concrete Structures*, John Wiley & Sons, 1975.

5. Kunnath, S. K., Reinhorn, A. M., and Abel, J. F., "A Computational Tool for Evaluation of Seismic Performance of Reinforced Concrete Building," *Computers & Structures*, Vol.41, No.1, 1990, pp.157~173.

6. Kunnath, S. K., Reinhorn, A. M., and Lobo, R. F., *IDARC Version 3.0: A Program for the Inelastic Damage Analysis of Reinforced Concrete Structures*, Technical Report, NCEER-92-0022, 1992.

7. Kunnath, S. K., Reinhorn, A. M., and Park, Y. J., "Analytical Modeling of Inelastic Seismic Response of R/C Structures," *Journal of Structural Engineering, ASCE*, Vol.16, No.4, 1990, pp.996~1017.

8. Roufaiel, M. S. L. and Meyer, C., "Analytical Modeling of Hysteretic Behavior of R/C Frames," *Journal of Structural Engineering, ASCE*, Vol.113, No.3, 1987, pp.429~444.

9. Stephens, J. E. and Yao, J. T. P., "Damage Assessment Using Response Measurements," *Journal of Structural Engineering, ASCEs*, Vol.113, No.4, 1987, pp.787~801.

10. Park, Y. J. and Ang, A. H. S., "Mechanistic Seismic Damage Model for Reinforced Concrete," *Journal of Structural Engineering, ASCE*, Vol.111, No.4, 1985, pp.722~739.